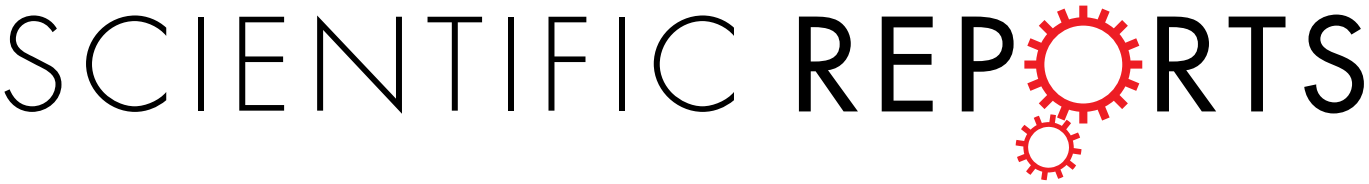

OPEN

Strain-induced nonlinear spin Hall effect in topological Dirac semimetal

Received: 30 May 2018
Accepted: 3 October 2018
Published online: 15 October 2018

Yasufumi Araki[1,2]

We show that an electric field applied to a strained topological Dirac semimetal, such as Na_3Bi and Cd_3As_2, induces a spin Hall current that is quadratic in the electric field. By regarding the strain as an effective "axial magnetic field" for the Dirac electrons, we investigate the electron and spin transport semiclassically in terms of the chiral kinetic theory. The nonlinear spin Hall effect arises as the cross effect between the regular Hall effect driven by the axial magnetic field and the anomalous Hall effect coming from the momentum-space topology. It provides an efficient way to generate a fully spin-polarized and rectified spin current out of an alternating electric field, which is sufficiently large and can be directly tuned by the gate voltage and the strain.

The idea of spin current, which first emerged about 50 years ago[1,2], has significantly developed the field of nanoscale condensed matter physics, in particular of spintronics[3–5]. Spin current plays an important role in controlling and detecting magnetization in magnetic nanostructures. The spin Hall effect (SHE) is one of the ways to obtain a spin current, in particular a pure spin current transverse to the injected charge current[6,7]. Its reciprocal effect, namely the inverse SHE (ISHE), converts the injected spin current into a charge current, which is useful in detecting a pure spin current[8,9]. The SHE is efficient in that it does not require any ferromagnetic material, which makes the system free from stray magnetic field.

The origin of the SHE can be classified into the extrinsic and intrinsic mechanisms. While the extrinsic mechanism is triggered by spin-asymmetric scattering at impurities with spin-orbit coupling (SOC)[10–12], the intrinsic effect originates from the nontrivial band topology due to SOC[13,14]. Since SOC violates the spin conservation, the spin current generated by the intrinsic SHE usually gets suppressed as it flows by a long distance. However, in some topological materials such as HgTe quantum well, the spin-orbit field (approximately) preserves U(1) spin symmetry by a certain quantization axis (e.g. S_z), yielding a spin Hall current that is fully polarized along the quantization axis. Its spin Hall conductivity is quantized, which is related to the $\mathbb{Z}_2$ topology of the eigenstate[15–17].

In three dimensions (3D), topological Dirac semimetals (TDSMs)[18,19], such as Na_3Bi[20] and Cd_3As_2[21], show the intrinsic SHE protected by $\mathbb{Z}_2$ topology. TDSMs are characterized by pair(s) of Dirac points (DPs/valleys) separated in momentum space, which are protected by rotational symmetry around an axis. The intrinsic spin Hall conductivity is determined by the separation of the DPs in momentum space[22–25], which is analogous to the anomalous Hall effect (AHE) in a Weyl semimetal (WSM) with broken time-reversal symmetry (TRS)[26,27]. The intrinsic SHE in TDSM is thus robust against disorders in bulk, and the value of spin Hall conductivity is fixed for each material.

Therefore, in order to tune and enhance the spin Hall current from its fixed value in TDSM, we need to go beyond the linear response regime with respect to the electric field, which is necessary in making use of TDSM as an efficient spin current injector. Nonlinear spin current generation is important for device application in that it generates a rectified (stationary) spin current from an alternating electric field, or a light, which has been proposed in transition metal dichalcogenides[28] and 2D Rashba–Dresselhaus systems[29]. Moreover, the nonlinear transport is important also from the topological point of view; a recent study has shown that the momentum-space Berry curvature gives rise to the nonlinear Hall transport[30]. For Dirac/Weyl semimetals, in particular, nonlinear charge current generation is proposed in several hypothetical setups, in which the strong Berry flux around the Dirac/Weyl points gives rise to the nonlinear current[31,32]. Nonlinear spin current generation might be of equal significance in Dirac/Weyl semimetals, although it has not been taken into account so far.

[1]Institute for Materials Research, Tohoku University, Sendai, 980-8577, Japan. [2]Frontier Research Institute for Interdisciplinary Sciences, Tohoku University, Sendai, 980-8578, Japan. Correspondence and requests for materials should be addressed to Y.A. (email: araki@imr.tohoku.ac.jp)

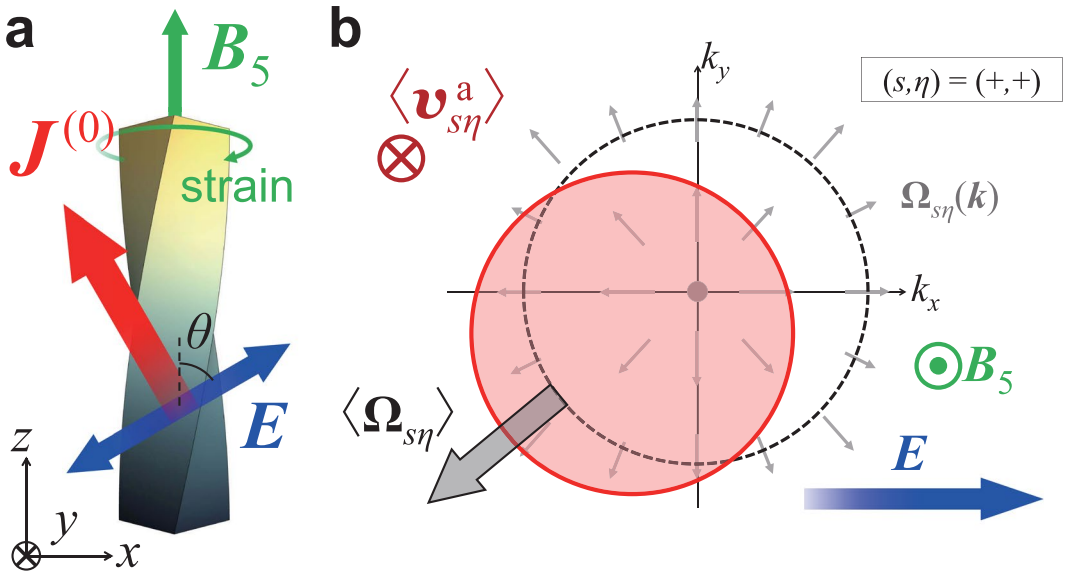

Figure 1. Schematic pictures for the nonlinear spin Hall effect in topological Dirac semimetal. (**a**) The setup of the system. A lattice strain on the topological Dirac semimetal (TDSM) is equivalent to the axial magnetic field $\mathbf{B}_5$. An alternating electric field $\mathbf{E}$ drives a rectified spin current $\mathbf{J}^{(0)}$ quadratic in $\mathbf{E}$. (**b**) The electron distribution in momentum space in response to the electric field $\mathbf{E}$ and the axial magnetic field $\mathbf{B}_5$. The distribution is shifted from the equilibrium distribution (dashed circle) transverse as well as longitudinal to $\mathbf{E}$ at linear response (red solid circle), due to the regular Hall effect (RHE) under $\mathbf{B}_5$. It induces an imbalance in the Berry curvature $\mathbf{\Omega}_{s\eta}$ (small grey arrows), which leads to the anomalous velocity $\mathbf{v}^a_{s\eta}$ as the second-order response in $\mathbf{E}$.

In this work, we demonstrate the nonlinear (quadratic) SHE in TDSM by introducing a lattice strain to the system. A lattice strain on a TDSM effectively serves as a valley-dependent magnetic field, namely the axial magnetic field[33–36], which is essential here in filtering the spin and valley degrees of freedom [see Fig. 1(a)]. We make use of the chiral kinetic theory, which describes the dynamics and distribution of the Dirac electrons for each valley[37–41], and derive the spin Hall current semiclassically up to the second order in the electric field. This nonlinear SHE can be regarded as the cross effect between the regular Hall effect (RHE) induced by the axial magnetic field and the AHE induced by the momentum-space topology[42–44]: the external electric field together with the axial magnetic field shifts the electron distribution in momentum space by the Lorentz force, and this shifted distribution yields the anomalous velocity due to the momentum-space Berry curvature, leading to the spin Hall current in total [see Fig. 1(b)]. We find that the nonlinear spin Hall current can be tuned by the gate voltage (electron chemical potential), and can reach the value comparable to the linear intrinsic spin Hall current, at the electric field ~10 kV/m. The spin current generated by this effect is fully spin-polarized and rectified even though the driving electric field is alternating, which we expect to be useful in designing TDSM-based spintronic devices.

Results

Topological Dirac semimetal and strain. We start with the low-energy effective Hamiltonian for TDSM,

$$H(\mathbf{k}) = v_F[\sigma_z\tau_x k_x - \tau_y k_y + \eta\tau_z(k_z - \eta k_D)], \tag{1}$$

with v_F the material-dependent Fermi velocity[18,19]. This minimal Hamiltonian consists of the atomic orbital degrees of freedom (e.g. Na-3*s* and Bi-6*p* for Na_3Bi) labeled by the Pauli matrix $\boldsymbol{\tau}$ and the spin (up/down) degrees of freedom labeled by $\boldsymbol{\sigma}$. The Hamiltonian is linearized around the two DPs, which reside at $\mathbf{k} = (0, 0, \eta k_D)$ with $\eta = \pm$ respectively. Each DP is doubly degenerate and is protected by the crystalline rotational symmetry around *z*-axis[22]. In the vicinity of the DPs, the energy eigenvaule for the electron (conduction) band is given as $\varepsilon(\mathbf{k}) = v_F|\mathbf{k} - \eta k_D\hat{\mathbf{e}}_z|$.

In the absence of nonlinear corrections in $\mathbf{k}$, σ_z behaves as a good quantum number, which we denote $s = \pm$ or spin up/down. For each $s = \pm$, the Hamiltonian takes the same form as that for a WSM with broken TRS. The topological charge for the valley η with spin s is $\nu_{s\eta} = s\eta$; the net topological charge cancels within each valley and within each spin[23]. This system shows the intrinsic SHE linear in the electric field, protected by the $\mathbb{Z}_2$ topology, with the spin Hall conductivity $\sigma^S_{xy} = (e^2/\pi^2)k_D$[25].

A lattice strain modifies this Hamiltonian, by altering the hopping terms among the orbitals. In general lattice systems, the effect of lattice strain is twofold; the longitudinal component of the strain tensor leads to renormalization of the hopping amplitudes, whereas the transverse part leads to new hopping terms that are allowed by breaking of the local crystalline symmetry[45]. These effects can be described as an effective vector potential in the continuum limit. In Dirac electron systems, such a strain-induced gauge field couples to each valley with the opposite sign (η) in the vicinity of the DPs, which is often referred to as an *axial* or *chiral* vector potential, to ensure TRS[33–36]. Such a correspondence is known in various crystalline systems such as graphene[46–48]. In TDSMs,

such as Na_3Bi and Cd_3As_2, a screw strain on a nanowire can generate an axial magnetic field $\mathbf{B}_5$ up to 0.3 T[34], and a bending of a thin film can make it up to 15 T[35]. In this work, we assume that $\mathbf{B}_5$ is macroscopically uniform for simplicity, and investigate the electron and spin transport up to the linear order in $\mathbf{B}_5$.

Field-induced current. In the present work, we focus on the electron transport driven by an electric field alternating with the frequency ω, defined by $\mathbf{E}(t) = 2\mathbf{E}_0 \cos\omega t$, which can account for a linearly polarized light as well. We omit the real magnetic field $\mathbf{B}$, whereas fix the strain-induced axial magnetic field $\mathbf{B}_5$ finite and (locally) homogeneous. Similarly to the real magnetic field, this axial magnetic field $\mathbf{B}_5$ gives rise to the Landau quantization, with the level spacing $\delta\varepsilon_{\rm LL} \sim v_{\rm F}\sqrt{2eB_5}$ at $k=0$. As long as the level spacing $\delta\varepsilon_{\rm LL}$ is lower than the Fermi level μ of the electrons, i.e. $\delta\varepsilon_{\rm LL} \lesssim |\mu|$, multiple Landau levels contribute to the electron transport, which implies that the transport can be well described by the semiclassical (Boltzmann) theory. By solving the Boltzmann equation for the electrons in terms of the chiral kinetic theory (see Methods), we estimate the driven current $\mathbf{j}_{s\eta}(t)$ for each spin s and valley η up to the first order in $\mathbf{B}_5$ and the second order in $\mathbf{E}_0$. While the linear response to the electric field $\mathbf{E}$ yields an alternating current $\mathbf{j}_{s\eta}^{(\pm\omega)}$, the quadratic response consists of the second harmonic part $\mathbf{j}_{s\eta}^{(\pm 2\omega)}$ and the stationary (rectified) part $\mathbf{j}_{s\eta}^{(0)}$, where the superscript with $(\cdot)$ on a physical quantity denotes its oscillation frequency.

Up to quadratic response to the electric field, we find that the stationary part $\mathbf{j}_{s\eta}^{(0)}$ depends only on the spin s but not on the valley η, namely $\mathbf{j}_{s\eta}^{(0)} \equiv (s/4)\mathbf{J}^{(0)}$. As a result, we obtain no net charge current but a pure spin current $\mathbf{J}^{(0)}$, with its quantization axis taken to S_z. This stationary spin current consists of the equilibrium part $\mathbf{J}_{\rm eq}^{(0)}$ that is independent of the electric field $\mathbf{E}_0$ and the nonequilibrium part $\mathbf{J}_{\rm neq}^{(0)}$ that is quadratic in $\mathbf{E}_0$. The equilibrium spin current

$$\mathbf{J}_{\rm eq}^{(0)} = -\frac{e^2}{\pi^2}\mu\mathbf{B}_5 \tag{2}$$

is the axial counterpart of the chiral magnetic effect, sometimes referred to as the *chiral axial magnetic* or *chiral pseudomagnetic effect*[49–51]. It comes from all the occupied states below the Fermi level, which is robust against disorder but cannot be taken out of the sample. On the other hand, the nonequilibrium part is given as

$$\mathbf{J}_{\rm neq}^{(0)} = -\frac{4e^2 v_{\rm F}^2}{3\pi^2\mu}\frac{\tau^2}{(1+\omega^2\tau^2)^2}(\mathbf{B}_5 \times \mathbf{E}_0) \times \mathbf{E}_0, \tag{3}$$

where τ is the relaxation time for all the relaxation processes, including the intravalley, intervalley, and spin-flip processes. This nonequilibrium spin current is carried by the electrons at the Fermi surface, and can be extracted out of the sample. Since this is the *spin* current that flows *perpendicular* to the electric field $\mathbf{E}_0$ and is *quadratic* in $\mathbf{E}_0$, we may call this effect the nonlinear spin Hall effect.

Origin of the nonlinear spin Hall effect. This nonlinear spin Hall current can be regarded as the interplay effect between the regular Hall effect (RHE) and the anomalous Hall effect (AHE) as follows: Fig. 1(b) shows its schematic picture. At the first order in the electric field, the Lorentz force by the axial magnetic field shifts the distribution $f_{s\eta}(\mathbf{k})$ for each spin s and valley η to the direction of $-\eta(\mathbf{B}_5 \times \mathbf{E})$, which accounts for the RHE. For each $\mathbf{k}$ in this shifted distribution, the anomalous velocity, which accounts for the intrinsic AHE in various TRS-broken systems, is given as $\mathbf{v}_{s\eta}^{\rm a} \sim \mathbf{E} \times \mathbf{\Omega}_{s\eta} \sim s\eta\mathbf{E} \times \hat{\mathbf{k}}$, using the $\mathbf{k}$-space Berry curvature $\mathbf{\Omega}_{s\eta}(\mathbf{k}) = s\eta\mathbf{k}/2k^3$ around each Dirac point. Integrating the anomalous velocity over the whole $\mathbf{k}$-space, its contribution to the current can be qualitatively estimated as

$$\mathbf{j}_{s\eta}^{\rm a} = -e\int\frac{d^3\mathbf{k}}{(2\pi)^3}\ \mathbf{v}_{s\eta}^{\rm a}(\mathbf{k})f_{s\eta}(\mathbf{k}) \sim -s\eta\mathbf{E} \times \int d^3\mathbf{k}\ \hat{\mathbf{k}}f_{s\eta}(\mathbf{k}) \sim s\mathbf{E} \times (\mathbf{B}_5 \times \mathbf{E}), \tag{4}$$

which accounts for the nonlinear spin Hall current given in Eq. (3). In this sense, we can regard the nonlinear SHE found here as the combination of the RHE and the AHE, or the interplay between the real-space topology and the momentum-space counterpart. [The Lorentz force for the RHE is imprinted in the second term in Eq. (8), while the anomalous velocity for the AHE appears in the second term in Eq. (7); see Methods for details].

How to detect the nonlinear spin Hall current. We are curious if the nonlinear spin Hall current obtained above can be observed experimentally. First, we estimate the typical magnitude of this spin current $\mathbf{J}_{\rm neq}^{(0)}$, by comparing it with other major spin currents, namely the equilibrium spin current $\mathbf{J}_{\rm eq}^{(0)}$ given by Eq. (2), and the linear intrinsic spin Hall current $\mathbf{J}_{\rm int}^{(\pm\omega)} = \sigma_{xy}^{\rm S}(\hat{\mathbf{e}}_z \times \mathbf{E}_0)$. As mentioned in Methods section, we explicitly supplement the linear intrinsic spin Hall current here, which is not included in the present chiral kinetic theory analysis. Although $\mathbf{J}_{\rm int}^{(\pm\omega)}$ driven by the AC electric field $\mathbf{E}(t)$ is alternating with the frequency ω, we shall compare it with the stationary spin currents to see which effect is the most dominant.

Using Eqs (2) and (3), the ratios among $\mathbf{J}_{\rm neq}^{(0)}$, $\mathbf{J}_{\rm eq}^{(0)}$, and $\mathbf{J}_{\rm int}^{(\pm\omega)}$ are given as

$$\frac{J_{\rm neq}^{(0)}}{J_{\rm eq}^{(0)}} = \frac{4}{3}\left(\frac{eE_0 v_{\rm F}\tau}{\mu Z_\omega}\right)^2, \quad \frac{J_{\rm neq}^{(0)}}{J_{\rm int}^{(\pm\omega)}} = \frac{4}{3}\frac{E_0 B_5}{\mu k_{\rm D}}\left(\frac{ev_{\rm F}\tau}{Z_\omega}\right)^2, \tag{5}$$

where $Z_\omega = 1+\omega^2\tau^2$. Here we employ the material parameters $v_{\rm F} = 0.5\times10^6$ m/s and $k_{\rm D} = 0.95\,{\rm nm}^{-1}$ observed in Na_3Bi[20], and use the typical values $\mu = 10$ meV and $\tau = 1$ ps. We introduce a lattice strain equivalent to the axial

magnetic field $B_5 = 0.3$ T, which satisfies the semiclassical condition $\delta\varepsilon_{\rm LL} \lesssim |\mu|$. Such a field can be generated in, for instance, a Cd_3As_2 nanowire that is twisted by the angle 180 degrees at the length ~1 μm[34]. In experimental studies, Cd_3As_2 nanowires of the diameter ~100 nm were found to be largely flexible against bending by 180 degrees[52,53], which implies that a nanowire may withstand the lattice strain generating such a large axial magnetic field. If an electric field $E_0 = 10^4$ V/m alternating in frequency $\omega \ll \tau^{-1}$ is applied to this system, the ratios among the induced currents are estimated as $J^{(0)}_{\rm neq}/J^{(0)}_{\rm eq} = 0.33$ and $J^{(0)}_{\rm neq}/J^{(\pm\omega)}_{\rm int} = 0.15$. From these ratios, we find that the nonlinear spin Hall current becomes sizable against the other two equilibrium spin currents under typical strengths of fields, which implies that the nonlinear spin Hall current is significant enough to be experimentally measured.

Next, let us check the orientation of the nonlinear spin Hall current and discuss how it can be detected experimentally. We define z-axis as the centre of strain, i.e. $\mathbf{B}_5 = B_5\hat{\mathbf{e}}_z$, and introduce the electric field $\mathbf{E}_0$ tilted from $\mathbf{B}_5$ by the angle θ, i.e. $\mathbf{E}_0 = \mathbf{E}_0(\cos\theta\,\hat{\mathbf{e}}_z + sin\,\theta\,\hat{\mathbf{e}}_x)$ [see Fig. 1(a)]. Then the nonlinear spin Hall current $\mathbf{J}^{(0)\rm neq}$ flows in parallel to

$$-(\mathbf{B}_5 \times \mathbf{E}_0) \times \mathbf{E}_0 = B_5 E_0^2 \sin\theta(\sin\theta\hat{\mathbf{e}}_z - \cos\theta\hat{\mathbf{e}}_x). \tag{6}$$

As we can easily see from this equation, the nonlinear spin Hall current vanishes when $\mathbf{E}_0 \| \mathbf{B}_5$ (i.e. $\theta = 0, \pi$). On the other hand, it is maximized when $\mathbf{E}_0 \perp \mathbf{B}_5$ (i.e. $\theta = \pi/2$), flowing in parallel to $\mathbf{B}_5$ (z-direction). If $\mathbf{E}_0$ is at the intermediate angle, the spin current flows in x-direction as well as z-direction.

The detection method of the spin current depends on its direction. The z-component of the spin current, flowing parallel to the screw strain axis, can be easily extracted from the system by putting a spin-sensitive material at the end of this axis. One can make use of a ferromagnetic metal or semiconductor, in which the injected spin current invokes a spin torque on the magnetization, leading to an oscillation or a switching of the magnetization. Heavy metals such as Pt can also be used, in which the spin current is converted to a charge current via the ISHE. On the other hand, the x-component of the spin current can be measured without any such external probes: the spin current flowing in x-direction can induce a charge current in y-direction via the (intrinsic) ISHE in the TDSM itself. Using the spin Hall angle $\theta_{\rm SH} = \sigma^{\rm S}_{xy}/\sigma_{xx}$, with σ_{xx} the in-plane longitudinal conductivity of the TDSM, the induced charge current can be given as $\mathbf{j}^{(0)}_{\rm ISH} = \theta_{\rm SH}\hat{\mathbf{e}}_z \times \mathbf{J}^{(0)}_{\rm neq}$. The θ-dependence shown in Eq. (6) may be checked by these measurements, with sweeping the direction of the **E**-field.

Discussion

In this work, we have focused on a strained TDSM (e.g. Na_3Bi, Cd_3As_2, etc.), and have demonstrated that such a system shows a significant nonlinear SHE, i.e. an external electric field induces a spin current perpendicular to the electric field as its quadratic response. This effect is described effectively by regarding the strain as the axial magnetic field $\mathbf{B}_5$, namely the valley-dependent magnetic field. The electron transport has been analysed semiclasically in terms of the chiral kinetic theory. The nonlinear SHE can be understood as the interplay effect between the RHE due to the axial magnetic field $\mathbf{B}_5$ and the AHE due to the finite Berry curvature in momentum space. This spin current reaches the magnitude comparable to the intrinsic spin Hall current under the electric field $\sim 10^4$ V/m, and can be successfully tuned via the gate voltage (electron chemical potential) and the strain (axial magnetic field). Our finding thus provides an efficient way to generate a rectified spin current out of an alternating electric field, which may be useful for spin injection in future spintronic devices.

Recent experiments successfully synthesized Cd_3As_2 nanowires with diameter of ~100 nm, which were found to be largely flexible against bending[52,53]. They also measured anomalous transport properties in those nanowires, namely the negative magnetoresistance arising from the chiral anomaly[52] and the Aharanov–Bohm oscillations in conductance dominated by the Fermi-arc surface states[53]. These findings imply that the band topology of TDSM strongly affects the electron transport properties even in the nanowire geometry, from which we can expect that the strain-induced nonlinear SHE proposed in the present article can be realized in such nanowire systems.

We have so far treated the disorder effect in terms of a single relaxation time τ for simplicity. However, in a realistic TDSM, the intravalley, intervalley, and spin-flipping scattering processes should be characterised by distinct relaxation times. In particular, it is known that the $O(k^3)$ terms that become significant away from the DPs violate the conservation of spin S_z, which give rise to the spin-flip process in the presence of strong scatterers. We leave the microscopic treatment of such scattering processes as an open question here.

As we have mentioned in the beginning, since there is no term that violates the spin symmetry by S_z around the DPs, each spin block (up/down) of the topological Dirac Hamiltonian can be regarded as the Weyl Hamiltonian with broken TRS. Extracting a single spin block out of our analysis, it can also account for the transport in TRS-broken WSMs. In particular, in magnetic WSMs (e.g. Mn_3Sn), an axial magnetic flux resides at a magnetic texture, such as magnetic domain walls, vortices, skyrmions, etc.[54], and its effect on the electronic spectrum has been verified both analytically and numerically[34,36,55]. In the presence of such an axial magnetic field, our analysis implies that there arises the nonlinear Hall effect, inducing a charge current. While the general theory of intrinsic nonlinear Hall effect was established in terms of the momentum-space Berry curvature in the recent literature[30], our setup also involves the real-space Berry curvature (axial magnetic field), to which their theory cannot be applied as it is. It will be another open question to find such theory with the Berry curvature involving the global phase space.

Methods

Chiral kinetic theory. In order to deal with the electron transport driven by the normal and axial electromagnetic fields, we first need to understand the dynamics of an electron wave packet. The dynamics of its centre-of-mass position $\boldsymbol{r}$ and its gauge-invariant momentum $\mathbf{k}$ measured from the DP is described by the semiclassical equations of motion[56–59],

$$\dot{\mathbf{r}} = \nabla_{\mathbf{k}}\tilde{\varepsilon}_{s\eta}(\mathbf{k}) - \dot{\mathbf{k}} \times \mathbf{\Omega}_{s\eta}(\mathbf{k}) \tag{7}$$

$$\dot{\mathbf{k}} = -e\mathbf{E}_{\eta} - e\dot{\mathbf{r}} \times \mathbf{B}_{\eta} \tag{8}$$

for each spin $s = \pm$ and valley $\eta = \pm$ [Note that $\mathbf{k}$ in these equations corresponds to $\mathbf{k} - \eta K\hat{\mathbf{e}}_z$ in Eq. (1)]. Here $\mathbf{E}_{\eta} = \mathbf{E} + \eta\mathbf{E}_5$ and $\mathbf{B}_{\eta} = \mathbf{B} + \eta\mathbf{B}_5$ denote the *effective* electromagnetic fields for each valley. Under the alternating electric field $\mathbf{E}(t) = 2\mathbf{E}_0 \cos\omega t$ and the lattice strain equivalent to the axial magnetic field $\mathbf{B}_5$, the effective electromagnetic fields are given by

$$\mathbf{E}_{\eta}(t) = \mathbf{E}_0(e^{i\omega t} + e^{-i\omega t}), \quad \mathbf{B}_{\eta} = \eta\mathbf{B}_5. \tag{9}$$

One should note that there are several modifications from the fully classical (Newtonian) equation of motion: the electron energy is modified from its band dispersion $\varepsilon(\mathbf{k})$ by the orbital magnetic moment $\mathbf{m}_{s\eta}(\mathbf{k})$ as $\tilde{\varepsilon}_{s\eta}(\mathbf{k}) = \varepsilon(\mathbf{k}) - \mathbf{m}_{s\eta}(\mathbf{k})\cdot\mathbf{B}_{\eta}$. The momentum-space Berry curvature $\mathbf{\Omega}_{s\eta}(\mathbf{k})$ gives rise to the anomalous velocity $-\dot{\mathbf{k}} \times \mathbf{\Omega}_{s\eta}$, which is the momentum-space counterpart of the Lorentz force $-e\dot{\mathbf{r}} \times \mathbf{B}_{\eta}$. In the electron band of the TDSM, i.e. for $\varepsilon(\mathbf{k}) = v_{\mathrm{F}}k$, the quantities mentioned above are given as

$$\mathbf{m}_{s\eta}(\mathbf{k}) = s\eta\frac{ev_{\mathrm{F}}}{2k}\hat{\mathbf{k}}, \quad \mathbf{\Omega}_{\eta}(\mathbf{k}) = s\eta\frac{1}{2k^2}\hat{\mathbf{k}}. \tag{10}$$

Since both of them are significant in the vicinity of the DPs, the nonlinear SHE discussed in this paper, which arises from these modifications, becomes stronger at lower Fermi level.

Based on the single-particle dynamics discussed above, we can describe the collective semiclassical dynamics of the electrons by the Boltzmann equation,

$$[\dot{\mathbf{r}} \cdot \nabla_{\mathbf{r}} + \dot{\mathbf{k}} \cdot \nabla_{\mathbf{k}} + \partial_t]f_{s\eta}(\mathbf{r}, \mathbf{k}, t) = \left(\frac{df_{s\eta}}{dt}\right)_{\mathrm{coll}} \tag{11}$$

for the electron distribution function $f_{s\eta}(\mathbf{r}, \mathbf{k}, t)$ for each spin s and valley η. The collision term $(df_{s\eta}/dt)_{\mathrm{coll}}$ consists of various scattering processes contributing to relaxation; here we approximate $(df_{s\eta}/dt)_{\mathrm{coll}} = -[f_{s\eta}(\mathbf{r}, \mathbf{k}, t) - f^{\mathrm{eq}}_{s\eta}(\mathbf{k})]/\tau$ with a single relaxation time τ for simplicity, with which we incorporate spin relaxation and intervalley scattering processes as well as the intravalley process[39]. $f^{\mathrm{eq}}_{s\eta}(\mathbf{k}) \equiv f^{\mathrm{eq}}(\tilde{\varepsilon}_{s\eta}(\mathbf{k}))$ is the equilibrium distribution modified by the orbital magnetization. Here we work with the chemical potential $\mu > 0$ in the zero-temperature limit, which gives $f^{\mathrm{eq}}(\varepsilon) = \theta(\mu - \varepsilon)$. We here require the spatial homogeneity of the system, so that the $\mathbf{r}$-dependence in $f_{s\eta}$ can be neglected.

By solving the kinetic equations [Eqs (7) and (8)] and the Boltzmann equation [Eq. (11)], the current for each spin and valley can be evaluated by

$$\mathbf{j}_{s\eta}(t) = -e\int\frac{d^3\mathbf{k}}{(2\pi)^3}D_{s\eta}(\mathbf{k})\dot{\mathbf{r}}f_{s\eta}(\mathbf{k}, t), \tag{12}$$

where $\dot{\mathbf{r}}$ is given as a function of $\mathbf{k}$ for each s and η by the solution of Eqs (7) and (8), and the factor $D_{s\eta}(\mathbf{k}) = 1 + e\mathbf{B}_{\eta}\cdot\mathbf{\Omega}_{s\eta}(\mathbf{k})$ accounts for the modification of the phase space volume. The net current, the spin current, and the valley current can be obtained by combining those $\{\mathbf{j}_{s\eta}\}$. We estimate the current up to the first order in $\mathbf{B}_5$ and the second order in $\mathbf{E}_0$; details of the solution process are shown in the Supplemental Material. We should note that the intrinsic spin Hall current linear in $\mathbf{E}$ is not included in this formulation, since the locations of the DPs are not taken into account. In the field theory description, it is described by the Chern–Simons (or Bardeen–Zumino) terms[40,51]. However, since we are primarily interested in the nonequilibrium current in response to the electric field, we first ignore it and later supplement it in the final discussion.

References

1. Dyakonov, M. I. & Perel, V. I. Possibility of Orienting Electron Spins with Current. *JETP Lett.* **13**, 467–469 (1971).
2. Dyakonov, M. I. & Perel, V. I. Current-induced spin orientation of electrons in semiconductors. *Phys. Lett. A* **35**, 459–460 (1971).
3. Žuti, I., Fabian, J. & Das Sarma, S. Spintronics: Fundamentals and applications. *Rev. Mod. Phys.* **76**, 323–410 (2004).
4. Edited by Maekawa, S., Valenzuela, S. O., Saitoh, E. & Kimura, T. *Spin Current* (Oxford University Press, New York, 2012).
5. Takahashi, S. & Maekawa, S. Spin current, spin accumulation and spin Hall effect. *Sci. Technol. Adv. Mater.* **9**, 014105, https://doi.org/10.1088/1468-6996/9/1/014105 (2008).
6. Edited by Dyakonov, M. I. *Spin Physics in Semiconductors* (Springer, 2008).
7. Sinova, J., Valenzuela, S. O., Wunderlich, J., Back, C. H. & Jungwirth, T. Spin Hall effects. *Rev. Mod. Phys.* **87**, 1213–1259 (2015).
8. Saitoh, E., Ueda, M., Miyajima, H. & Tatara, G. Conversion of spin current into charge current at room temperature: Inverse spin-Hall effect. *Appl. Phys. Lett.* **88**, 182509, https://doi.org/10.1063/1.2199473 (2006).
9. Valenzuela, S. O. & Tinkham, M. Direct electronic measurement of the spin Hall effect. *Nature* **442**, 176–179 (2006).
10. Dyakonov, M. & Perel, V. I. Spin Orientation of Electrons Associated with the Interband Absorption of Light in Semiconductors. *JETP* **33**, 1053–1059 (1971).
11. Hirsch, J. E. Spin Hall Effect. *Phys. Rev. Lett.* **83**, 1834–1837 (1999).
12. Zhang, S. Spin Hall Effect in the Presence of Spin Diffusion. *Phys. Rev. Lett.* **85**, 393–396 (2000).
13. Murakami, S., Nagaosa, N. & Zhang, S.-C. Dissipationless Quantum Spin Current at Room Temperature. *Science* **301**, 1348–1351 (2003).
14. Sinova, J. *et al.* Universal Intrinsic Spin Hall Effect. *Phys. Rev. Lett.* **92**, 126603, https://doi.org/10.1103/PhysRevLett.92.126603 (2004).

15. Murakami, S., Nagaosa, N. & Zhang, S.-C. Spin-Hall Insulator. *Phys. Rev. Lett.* **93**, 156804, https://doi.org/10.1103/PhysRevLett.93.156804 (2004).
16. Kane, C. L. & Mele, E. J. Z_2 Topological Order and the Quantum Spin Hall Effect. *Phys. Rev. Lett.* **95**, 146802, https://doi.org/10.1103/PhysRevLett.95.146802 (2005).
17. Bernevig, B. A., Hughes, T. L. & Zhang, S.-C. Quantum Spin Hall Effect and Topological Phase Transition in HgTe Quantum Wells. *Science* **314**, 1757–1761 (2006).
18. Wang, Z. *et al.* Dirac semimetal and topological phase transitions in A_3Bi (A = Na, K, Rb). *Phys. Rev. B* **85**, 195320, https://doi.org/10.1103/PhysRevB.85.195320 (2012).
19. Wang, Z., Weng, H., Wu, Q., Dai, X. & Fang, Z. Three-dimensional Dirac semimetal and quantum transport in Cd_3As_2. *Phys. Rev. B* **88**, 125427, https://doi.org/10.1103/PhysRevB.88.125427 (2013).
20. Liu, Z. K. *et al.* Discovery of a Three-Dimensional Topological Dirac Semimetal, Na_3Bi. *Science* **343**, 864–867 (2014).
21. Neupane, M. *et al.* Observation of a three-dimensional topological Dirac semimetal phase in high-mobility Cd_3As_2. *Nat. Commun.* **5**, 3786, https://doi.org/10.1038/ncomms4786 (2014).
22. Yang, B.-J. & Nagaosa, N. Classification of stable three-dimensional Dirac semimetals with nontrivial topology. *Nat. Commun.* **5**, 4898, https://doi.org/10.1038/ncomms5898 (2014).
23. Yang, B.-J., Morimoto, T. & Furusaki, A. Topological charges of three-dimensional Dirac semimetals with rotation symmetry. *Phys. Rev. B* **92**, 165120, https://doi.org/10.1103/PhysRevB.92.165120 (2015).
24. Gorbar, E. V., Miransky, V. A., Shovkovy, I. A. & Sukhachov, P. O. Dirac semimetals A_3Bi (A = Na, K, Rb) as Z_2 Weyl semimetals. *Phys. Rev. B* **91**, 121101, https://doi.org/10.1103/PhysRevB.91.121101 (2015).
25. Burkov, A. A. & Kim, Y. B. Z_2 and Chiral Anomalies in Topological Dirac Semimetals. *Phys. Rev. Lett.* **117**, 136602, https://doi.org/10.1103/PhysRevLett.117.136602 (2016).
26. Burkov, A. A. & Balents, L. Weyl Semimetal in a Topological Insulator Multilayer. *Phys. Rev. Lett.* **107**, 127205, https://doi.org/10.1103/PhysRevLett.107.127205 (2011).
27. Yang, K.-Y., Lu, Y.-M. & Ran, Y. Quantum Hall effects in a Weyl semimetal: Possible application in pyrochlore iridates. *Phys. Rev. B* **84**, 075129, https://doi.org/10.1103/PhysRevB.84.075129 (2011).
28. Yu, H., Wu, Y., Liu, G.-B., Xu, X. & Yao, W. Nonlinear Valley and Spin Currents from Fermi Pocket Anisotropy in 2D Crystals. *Phys. Rev. Lett.* **113**, 156603, https://doi.org/10.1103/PhysRevLett.113.156603 (2014).
29. Hamamoto, K., Ezawa, M., Kim, K. W., Morimoto, T. & Nagaosa, N. Nonlinear spin current generation in noncentrosymmetric spin-orbit coupled systems. *Phys. Rev. B* **95**, 224430, https://doi.org/10.1103/PhysRevB.95.224430 (2017).
30. Sodemann, I. & Fu, L. Quantum Nonlinear Hall Effect Induced by Berry Curvature Dipole in Time-Reversal Invariant Materials. *Phys. Rev. Lett.* **115**, 216806, https://doi.org/10.1103/PhysRevLett.115.216806 (2015).
31. Morimoto, T., Zhong, S., Orenstein, J. & Moore, J. E. Semiclassical theory of nonlinear magneto-optical responses with applications to topological Dirac/Weyl semimetals. *Phys. Rev. B* **94**, 245121, https://doi.org/10.1103/PhysRevB.94.245121 (2016).
32. Zyuzin, A. A. & Zyuzin, A. Yu. Chiral anomaly and second-harmonic generation in Weyl semimetals. *Phys. Rev. B* **95**, 085127, https://doi.org/10.1103/PhysRevB.95.085127 (2017).
33. Cortijo, A., Ferreirós, Y., Landsteiner, K. & Vozmediano, M. A. H. Elastic Gauge Fields in Weyl Semimetals. *Phys. Rev. Lett.* **115**, 177202, https://doi.org/10.1103/PhysRevLett.115.177202 (2015).
34. Pikulin, D. I., Chen, A. & Franz, M. Chiral Anomaly from Strain-Induced Gauge Fields in Dirac and Weyl Semimetals. *Phys. Rev. X* **6**, 041021, https://doi.org/10.1103/PhysRevX.6.041021 (2016).
35. Liu, T., Pikulin, D. I. & Franz, M. Quantum oscillations without magnetic field. *Phys. Rev. B* **95**, 041201, https://doi.org/10.1103/PhysRevB.95.041201 (2017).
36. Grushin, A. G., Venderbos, J. W. F., Vishwanath, A. & Ilan, R. Inhomogeneous Weyl and Dirac Semimetals: Transport in Axial Magnetic Fields and Fermi Arc Surface States from Pseudo-Landau Levels. *Phys. Rev. X* **6**, 041046, https://doi.org/10.1103/PhysRevX.6.041046 (2016).
37. Stephanov, M. A. & Yin, Y. Chiral Kinetic Theory. *Phys. Rev. Lett.* **109**, 162001, https://doi.org/10.1103/PhysRevLett.109.162001 (2012).
38. Son, D. T. & Yamamoto, N. Kinetic theory with Berry curvature from quantum field theories. *Phys. Rev. D* **87**, 085016, https://doi.org/10.1103/PhysRevD.87.085016 (2013).
39. Son, D. T. & Spivak, B. Z. Chiral anomaly and classical negative magnetoresistance of Weyl metals. *Phys. Rev. B* **88**, 104412, https://doi.org/10.1103/PhysRevB.88.104412 (2013).
40. Gorbar, E. V., Miransky, V. A., Shovkovy, I. A. & Sukhachov, P. O. Consistent Chiral Kinetic Theory in Weyl Materials: Chiral Magnetic Plasmons. *Phys. Rev. Lett.* **118**, 127601, https://doi.org/10.1103/PhysRevLett.118.127601 (2017).
41. Zyuzin, V. A. Magnetotransport of Weyl semimetals due to the chiral anomaly. *Phys. Rev. B* **95**, 245128, https://doi.org/10.1103/PhysRevB.95.245128 (2017).
42. Karplus, R. & Luttinger, J. M. Hall Effect in Ferromagnetics. *Phys. Rev.* **95**, 1154–1160 (1954).
43. Jungwirth, T., Niu, Q. & MacDonald, A. H. Anomalous Hall Effect in Ferromagnetic Semiconductors. *Phys. Rev. Lett.* **88**, 207208, https://doi.org/10.1103/PhysRevLett.88.207208 (2002).
44. Onoda, M. & Nagaosa, N. Topological Nature of Anomalous Hall Effect in Ferromagnets. *J. Phys. Soc. Jpn.* **71**, 19–22 (2002).
45. Shapourian, H., Hughes, T. L. & Ryu, S. Viscoelastic response of topological tight-binding models in two and three dimensions. *Phys. Rev. B* **92**, 165131, https://doi.org/10.1103/PhysRevB.92.165131 (2015).
46. González, J., Guinea, F. & Vozmediano, M. A. H. Continuum approximation to fullerene molecules. *Phys. Rev. Lett.* **69**, 172–175 (1992).
47. Suzuura, H. & Ando, T. Phonons and electron-phonon scattering in carbon nanotubes. *Phys. Rev. B* **65**, 235412, https://doi.org/10.1103/PhysRevB.65.235412 (2002).
48. Guinea, F., Katsnelson, M. I. & Geim, A. K. Energy gaps and a zero-field quantum Hall effect in graphene by strain engineering. *Nat. Phys.* **6**, 30–33 (2010).
49. Zhou, J.-H., Jiang, H., Niu, Q. & Shi, J.-R. Topological Invariants of Metals and the Related Physical Effects. *Chin. Phys. Lett.* **30**, 027101, https://doi.org/10.1088/0256-307X/30/2/027101 (2012).
50. Huang, Z.-M., Zhou, J. & Shen, S.-Q. Topological responses from chiral anomaly in multi-Weyl semimetals. *Phys. Rev. B* **96**, 085201, https://doi.org/10.1103/PhysRevB.96.085201 (2017).
51. Gorbar, E. V., Miransky, V. A., Shovkovy, I. A. & Sukhachov, P. O. Origin of Bardeen-Zumino current in lattice models of Weyl semimetals. *Phys. Rev. B* **96**, 085130, https://doi.org/10.1103/PhysRevB.96.085130 (2017).
52. Li, C.-Z. *et al.* Giant negative magnetoresistance induced by the chiral anomaly in individual Cd_3As_2 nanowires. *Nat. Commun.* **6**, 10137, https://doi.org/10.1038/ncomms10137 (2015).
53. Wang, L.-X., Li, C.-Z., Yu, D.-P. & Liao, Z.-M. Aharonov–Bohm oscillations in Dirac semimetal Cd_3As_2 nanowires. *Nat. Commun.* **7**, 10769, https://doi.org/10.1038/ncomms10769 (2016).
54. Liu, C.-X., Ye, P. & Qi, X.-L. Chiral gauge field and axial anomaly in a Weyl semimetal. *Phys. Rev. B* **87**, 235306, https://doi.org/10.1103/PhysRevB.87.235306 (2013).
55. Araki, Y., Yoshida, A. & Nomura, K. Universal charge and current on magnetic domain walls in Weyl semimetals. *Phys. Rev. B* **94**, 115312, https://doi.org/10.1103/PhysRevB.94.115312 (2016).
56. Chang, M.-C. & Niu, Q. Berry Phase, Hyperorbits, and the Hofstadter Spectrum. *Phys. Rev. Lett.* **75**, 1348–1351 (1995).

57. Chang, M.-C. & Niu, Q. Berry phase, hyperorbits, and the Hofstadter spectrum: Semiclassical dynamics in magnetic Bloch bands. *Phys. Rev. B* **53**, 7010–7023 (1996).
58. Sundaram, G. & Niu, Q. Wave-packet dynamics in slowly perturbed crystals: Gradient corrections and Berry-phase effects. *Phys. Rev. B* **59**, 14915–14925 (1999).
59. Xiao, D., Chang, M.-C. & Niu, Q. Berry phase effects on electronic properties. *Rev. Mod. Phys.* **82**, 1959–2007 (2010).

Acknowledgements

This work is supported by JSPS KAKENHI Grant Number JP17K14316. The author acknowledges K. Kobayashi, K. Nomura, and Y. Ominato for fruitful discussions.

Author Contributions

The author carried out all the theoretical analysis and the preparation of the manuscript.

Additional Information

Supplementary information accompanies this paper at https://doi.org/10.1038/s41598-018-33655-w.

Competing Interests: The author declares no competing interests.

Publisher's note: Springer Nature remains neutral with regard to jurisdictional claims in published maps and institutional affiliations.